university of groningen

University Medical Center Groningen

University of Groningen

Sub-LET Threshold SEE cross section dependency with ion energy

Garcia Alia, Ruben; Bahamonde, C.; Brandenburg, Sijtze; Brugger, Markus; Daly, E.; Ferlet-Cavrois, Veronique; Gaillard, R.; Hoeffgen, S. ; Menicucci, A.; Metzger, S.

Published in:
IEEE Transactions on Nuclear Science

DOI:
10.1109/TNS.2015.2483021

IMPORTANT NOTE: You are advised to consult the publisher's version (publisher's PDF) if you wish to cite from it. Please check the document version below.

Document Version
Publisher's PDF, also known as Version of record

Publication date:
2015

Link to publication in University of Groningen/UMCG research database

Citation for published version (APA):
Garcia Alia, R., Bahamonde, C., Brandenburg, S., Brugger, M., Daly, E., Ferlet-Cavrois, V., Gaillard, R., Hoeffgen, S., Menicucci, A., Metzger, S., Zadeh, A., Muschitiello, M., Noordeh, A., & Santin, G. (2015). Sub-LET Threshold SEE cross section dependency with ion energy. *IEEE Transactions on Nuclear Science*, *62*(6), 2797-2806. https://doi.org/10.1109/TNS.2015.2483021

Copyright
Other than for strictly personal use, it is not permitted to download or to forward/distribute the text or part of it without the consent of the author(s) and/or copyright holder(s), unless the work is under an open content license (like Creative Commons).

The publication may also be distributed here under the terms of Article 25fa of the Dutch Copyright Act, indicated by the “Taverne” license. More information can be found on the University of Groningen website: https://www.rug.nl/library/open-access/self-archiving-pure/taverne-amendment.

Take-down policy
If you believe that this document breaches copyright please contact us providing details, and we will remove access to the work immediately and investigate your claim.

Downloaded from the University of Groningen/UMCG research database (Pure): http://www.rug.nl/research/portal. For technical reasons the number of authors shown on this cover page is limited to 10 maximum.

Download date: 05-06-2022

Sub-LET Threshold SEE Cross Section Dependency With Ion Energy

Rubén García Alía, Cristina Bahamonde, Sytze Brandenburg, Markus Brugger, Eamonn Daly, Véronique Ferlet-Cavrois, Rémi Gaillard, Stefan Hoeffgen, Alessandra Menicucci, Stefan Metzger, Ali Zadeh, Michele Muschitiello, Emil Noordeh, and Giovanni Santin

***Abstract*—This study focuses on the ion species and energy dependence of the heavy ion SEE cross section in the sub-LET threshold region through a set of experimental data. In addition, a Monte Carlo based model is introduced and applied, showing a good agreement with the data in the several hundred MeV/n range while evidencing large discrepancies with the measurements in the 10-30 MeV/n interval, notably for the Ne ion. Such discrepancies are carefully analyzed and discussed.**

***Index Terms*—FLUKA, indirect ionization, Monte Carlo methods, nuclear reactions, single-event burnout (SEB), single-event upset (SEU).**

I. Introduction

SIMILARLY to protons and neutrons, heavy ions have long been known capable of inducing Single Event Effects (SEEs) through indirect energy deposition events [1]. These events, product of nuclear reactions, are experimentally visible in the so-called sub-Linear Energy Transfer (LET) threshold region, in which the primary ions have LET values too low to induce SEEs through direct ionization. In fact, as was predicted through calculations in [2], [3] and measured in-orbit in [4], the contribution from heavy ion induced nuclear reactions can be dominant (by over two orders of magnitude) for an interplanetary environment and a radiation hardened component with respect to the traditional, direct ionization based prediction methods.

Quantifying the nuclear reaction contribution is therefore essential in order to obtain realistic in-orbit SEE rate calculations, notably for components hardened by design or commercial devices intrinsically having a large LET threshold value. However, provided the very broad range of ion species and energies present in the Galactic Cosmic Rays (GCR) it is not feasible to experimentally characterize components in the full relevant phase space, and therefore alternative methods of estimating the on-board failure rate need to be investigated. One of the possible solutions is to perform calculations using Monte Carlo simulations that account for the transport and interaction of the ions through matter based on the respective physical laws. However, the authors of [4] point out that, in the sub-LET threshold domain (in which indirect energy deposition events are responsible for SEEs), simulation tools provide less accurate results than in the above-threshold region. In particular, a very large discrepancy is reported for one SRAM and a 40 MeV/n ^{40}Ar ion in TAMU at Texas A&M [5], for which the simulated sub-LET threshold cross section value was roughly two orders of magnitude below the experimental result.

Therefore, the aim of the present study is to analyze the dependency of the Single Event Upset (SEU) cross section with the ion species and energy in the sub-LET threshold region and evaluate the potential discrepancy between experimental data and simulations. The analysis is first based on test results on one component (the European Space Agency (ESA) SEU Monitor) in five different test facilities, and adds to previous work by including experimental and simulated results of (i) sub-LET threshold measurements at energies up to 1.5 GeV/n and (ii) the recently available KVI Heavy Ion (HI) facility in the University of Groningen, the Netherlands, covering a similar energy range as TAMU.

Simulations are performed using the FLUKA Monte Carlo code [6]–[8] and considering an IRPP-based model. In addition, sub-LET threshold experimental results are also shown for Single Event Burnout (SEB) in a power MOSFET. This case is of particular relevance for hardness assurance of components to be flown in space as (i) it involves a potentially destructive failure and (ii) the LET threshold for the device and failure is such that nuclear reactions could have a very strong contribution to the overall failure rate.

II. Heavy Ion Measurements

The ESA SEU Monitor is an SRAM-based radiation detector which has been characterized in a broad range of facilities and can therefore be used as a so-called golden chip in order to measure the beam intensity and homogeneity in an experimental context [9]–[12]. HI tests were performed by ESA on the SEU Monitor in five different test facilities covering an LET range

Manuscript received July 10, 2015; revised September 15, 2015; accepted September 16, 2015. Date of current version December 11, 2015.

R. García Alía and M. Brugger are with CERN, CH-1211, Genève, Switzerland (e-mail ruben.garcia.alia@cern.ch).

C. Bahamonde is with the University of Utah, Salt Lake City, UT 84112, USA.

S. Brandenburg is with the KVI-Center for Advance Radiation Technology (CART), University of Groningen, 9747 AA Groningen, The Netherlands.

E. Daly, V. Ferlet-Cavrois, A. Menicucci, A. Zadeh, M. Muschitiello, and G. Santin are with the European Space Agency, ESTEC, 2200 AG Noordwijk, The Netherlands.

R. Gaillard is at 78730 Saint-Arnoult, France.

S. Hoeffgen and S. Metzger are with the Fraunhofer INT, 53879 Euskirchen, Germany.

E. Nordeeh is with York University, Toronto, ON M3J 1P3, Canada.

Color versions of one or more of the figures in this paper are available online at http://ieeexplore.ieee.org.

Digital Object Identifier 10.1109/TNS.2015.2483021

0018-9499 © 2015 IEEE. Personal use is permitted, but republication/redistribution requires IEEE permission.
See http://www.ieee.org/publications_standards/publications/rights/index.html for more information.

Authorized licensed use limited to: University of Groningen. Downloaded on October 02,2020 at 07:56:07 UTC from IEEE Xplore. Restrictions apply.

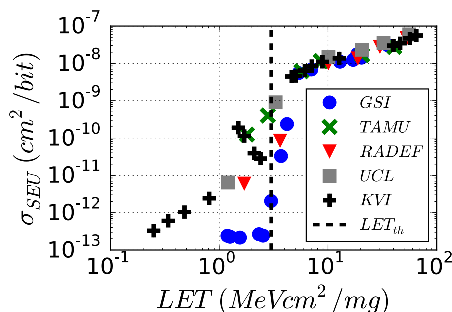

Fig. 1. Heavy ion test data as a function of LET.

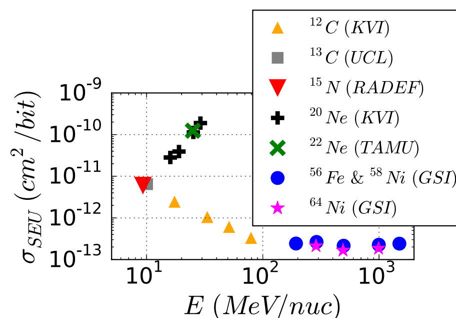

Fig. 2. Sub-threshold heavy ion test data as a function of energy per nucleon.

of $\sim$ 1 − 65 MeV cm^2/mg and an energy range of $\sim$ 10 − 1500 MeV/n. Details about the measurements are provided in [13], [14]. The facilities used were RADEF, UCL, TAMU, GSI and KVI and the set of cross section measurements as a function of LET is shown in Fig. 1 per facility, only including data taken at normal incidence. An LET threshold of 3 MeV cm^2/mg is considered as we will later justify.

As can be seen, data points above $\sim$ 4.5 MeV cm^2/mg clearly follow the same trend regardless of the test facility, as expected for processes where LET is representative of SEU probability. The region near threshold ($\sim$ 2.6 − 4.5 MeV cm^2/mg) exhibits an abrupt decrease with LET while showing a significant spread among different facilities. As is shown in detail in [14], this spread is also observed among data corresponding to the same facility and different individual components (which are merged here for simplification) and is therefore mainly attributed to the spread in the sensitivity of the different components tested. The uncertainty on the actual LET value when the ions reach the SV might also play an important role. Due to the very strong dependency of the cross section with LET in this interval, small changes in these values can lead to very large variations in the experimental cross section. Finally, in the sub-LET threshold region ($<$ 2.6 MeV cm^2/mg) differences of up to three orders of magnitude can be noticed for ions with the same (or very similar) LET values but corresponding to different facilities and thus ions and energies. As we will show later, the same two data sets that showed large discrepancies for the same (or very similar) ion and energy at GSI in the near-threshold region are fully consistent in the sub-LET threshold range, thus strengthening the arguments linking the observed spread amongst the data to the difference in the actual LET threshold of individual components, and which has a negligible impact on the sub-LET threshold results.

As has been broadly discussed in the past ([3] and references therein), SEUs in the sub-LET threshold region are by definition not induced through direct ionization of the incident ion, but are rather attributed to nuclear fragments from its interactions with the nuclei in the Sensitive Volume (SV) and its surroundings. Therefore, LET is no longer a relevant quantity to describe the SEU probability in this region, and the ion energy per nucleon is used instead provided the reaction probability has a relatively regular dependence on it. For this reason, the sub-LET threshold experimental data considered in this work are detailed in Table I in ascending energy per nucleon. Results are plotted in Fig. 2 also as a function of the energy per nucleon. It is to be noted

TABLE I
SUB-LET THRESHOLD ESA MONITOR SEU HEAVY ION DATA. MORE THAN 1000 SEUS WERE OBTAINED PER EXPERIMENTAL POINT, THEREFORE STATISTICAL ERROR BARS ARE NOT CONSIDERED IN THE PLOTS

Facility	Ion	Energy (MeV/n)	LET (MeVcm^2/mg)	σ_{SEU} (cm^2/bit)
RADEF	^{15}N	9.3	1.7	$6.04 \cdot 10^{-12}$
UCL	^{13}C	10	1.2	$6.44 \cdot 10^{-12}$
KVI	^{20}Ne	16	2.4	$2.82 \cdot 10^{-11}$
	^{12}C	17.4	0.81	$2.43 \cdot 10^{-12}$
	^{20}Ne	19	2.1	$3.92 \cdot 10^{-11}$
	^{20}Ne	25	1.7	$1.13 \cdot 10^{-10}$
TAMU	^{22}Ne	25	1.8	$1.24 \cdot 10^{-10}$
KVI	^{20}Ne	29	1.5	$1.89 \cdot 10^{-10}$
KVI	^{12}C	33.3	0.48	$1.02 \cdot 10^{-12}$
	^{12}C	51.3	0.34	$6.04 \cdot 10^{-12}$
	^{12}C	79.2	0.25	$3.28 \cdot 10^{-13}$
GSI	^{56}Fe	190	2.5	$2.43 \cdot 10^{-13}$
	^{58}Ni	290	2.3	$2.65 \cdot 10^{-13}$
	^{64}Ni	290	2.3	$2.13 \cdot 10^{-13}$
	^{64}Ni	490	1.8	$1.67 \cdot 10^{-13}$
	^{56}Fe	500	1.6	$2.15 \cdot 10^{-13}$
	^{64}Ni	1000	1.5	$1.86 \cdot 10^{-13}$
	^{56}Fe	1000	1.3	$2.27 \cdot 10^{-13}$
	^{56}Fe	1500	1.2	$2.41 \cdot 10^{-13}$

that, whereas the plot aims at highlighting the dependency of the cross section with energy, the data points correspond to different data species as marked in the legend. Beams at KVI used a primary beam of 30 MeV/n for Ne and 90 MeV/n for C, and as will be shown in detail in Section VI were degraded down to the energies reported in Table I.

As can be seen in Fig. 2, a significant cross section increase with energy is observed in the 10-30 MeV/n range for the Ne ion, in line with what was previously presented and discussed in [15]. It is worth noting that data in this interval includes an overlap between RADEF and UCL at around 10 MeV/n and TAMU and KVI at around 25 MeV/n. In both cases, the respective cross sections are fully compatible. In contrast, for the C ion, the cross section decreases gradually between 10 and 80 MeV/n, thus exhibiting a clearly different behavior than Ne while having similar atomic and mass numbers. Furthermore, the cross section values in the 200-1500 MeV/n range are fairly constant with energy at a value significantly lower than results in the 10-30 MeV/n range for Ne, and compatible with the decreasing trend of the C ion. It is also worth noting that the ^{56}Fe/^{58}Ni and ^{64}Ni data sets (not included in Fig. 1 in order to avoid overloading the plot) correspond to two different DUTs

Authorized licensed use limited to: University of Groningen. Downloaded on October 02,2020 at 07:56:07 UTC from IEEE Xplore. Restrictions apply.

which as was mentioned above showed significant discrepancies in the LET threshold region, but are fully compatible in the sub-LET threshold interval.

III. SEU Model Calibration and Benchmark

In order to further explore the energy and ion species dependency in the sub-LET threshold region, we make use of the FLUKA Monte Carlo simulation code [6]–[8] to calculate the transport, interaction and energy deposition of the ions in the device's SV and its surroundings. For this purpose, we use technological information about the SRAM transistor technology in order to define the surface sensitive to the charge collection as that corresponding to an individual SRAM cell ($\sim 10\ \mu\text{m}^2$). As to what regards the thickness of the SV, we consider 0.5 μm in line with what has been published in studies on similar technologies [16]. As we will later quantify, the variations of this parameter within reasonable margins do not have a significant impact on the simulation outcome.

Once the SV is defined, we consider that the probability of inducing an SEU does not directly depend on the energy deposited in the SV but rather on the charge collected in the sensitive node. The relationship between both can be described through the charge collection efficiency (CCE), representing the proportion of charge collected as a function of the path within the SRAM cell [17]. The different CCE factors can be considered through the definition of nested volumes with decreasing charge collection efficiencies as their distance to the sensitive drain increases [18], [19]. In the present work however, we consider that the probability of a certain energy deposition to lead to an SEU can be described through the device's heavy ion cross section as a function of deposited energy in the range in which direct ionization is the dominating effect (i.e. in the above-threshold region). This response function represents the probability that an ion of a given LET will have a trajectory such that enough energy is collected in the sensitive node to generate the SEU, thus effectively considering the CCE distribution represented by the response function (i.e. in a similar way as performed in the integral rectangular parallelepiped (IRPP) analytic approach for in-orbit SEE rate predictions [20]).

Instead of directly using the fit to the experimental SEU cross section as the response function of the device, we use the SV introduced above ($10\ \mu\text{m}^2 \times 0.5\ \mu\text{m}$) together with its Back-End-Of-Line (BEOL, 6.7 μm of aluminum and silicon dioxide layers according to information provided by the SRAM manufacturer) to simulate the above-threshold experimental points shown in Fig. 1. Only data up to 20 MeV cm^2/mg is considered, as the behavior of the cross section above this LET is not compatible with a saturated Weibull function (see Fig. 1) and is therefore attributed to the induction of Multiple Cell Upsets (MCUs) which are not included in our model. We then find the best fit to the four Weibull parameters in Eq. (1), where E is the deposited energy, σ_{sat} is the saturation cross section, E_o is the threshold energy and s and W are the shape parameters.

The respective best-fit values are reported in Table II. Although experimental cross section values are shown as a function of LET, simulations provide energy deposition distributions as a result. These distributions are converted to LET through the considered thickness (in this case, 0.5 μm). The resulting

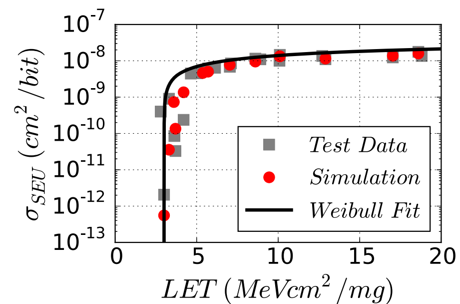

Fig. 3. Response function that optimizes the fit of the simulated values to the test data.

TABLE II
Fit Parameters of the ESA SEU Monitor Response Curve

Parameter	Value
σ_{sat}	$3.72 \cdot 10^{-8}$ cm^2
E_o	0.35 MeV
w	2.53 MeV
s	0.66

Weibull function that optimizes the fit between simulated and experimental data is shown in Fig. 3 together with the two latter values. The reason why the simulated data do not directly lie on the response curve is that the simulated deposited energy is not a unique value equal to the LET times the thickness but rather follows a certain distribution which will depend on factors such as the spread in the ion energy, fluctuations in the energy deposition, etc. Likewise, whereas LET considers the total energy loss of the ion through ionization, the energy deposition accounts only for the fraction of energy deposited within a certain volume

$$\sigma(\text{E}) = \sigma_{\text{sat}} \cdot (1 - \text{e}^{-((\text{E}-\text{E}_\text{o})/\text{W})^{\text{s}}}). \quad (1)$$

Once the heavy ion response function is calibrated, it can be used to calculate the SEU cross section for indirect energy deposition events by folding it with the respective energy deposition distribution. An example of such a mechanism are SEUs induced by protons, which for the technology here considered can only be triggered through the products of their nuclear reactions with the SV and its surroundings. This formalism, while analogous to that originally introduced in the SIMPA approach [21], [22] or proposed by Barak and others [23], is based on up-to-date nuclear interaction models and allows for a more flexible definition of the SV dimensions and its surrounding materials.

As the ESA Monitor response to protons has been extensively characterized, we use the Monte Carlo simulations of the deposited energy distributions and the response function introduced above to simulate the proton cross section as a function of energy and benchmark it against the measurements. As is shown in Fig. 4, the model is highly successful in reproducing the experimental proton data. It is important to note at this stage that the model used, while being empirically calibrated to the above-threshold heavy ion data, is fully independent of the proton data (i.e. no further parameter is adjusted to it). Likewise, it is relevant to state that the dependence of the

Authorized licensed use limited to: University of Groningen. Downloaded on October 02,2020 at 07:56:07 UTC from IEEE Xplore. Restrictions apply.

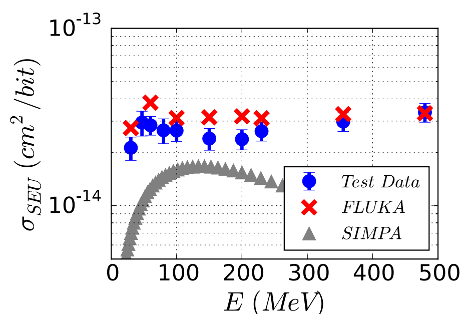

Fig. 4. Experimental and simulated ESA Monitor SEU proton cross section data obtained at PSI and TRIUMF [25] for an SV thickness of 0.5 μm. The output from the SIMPA model using the same response function and SV thickness is also included.

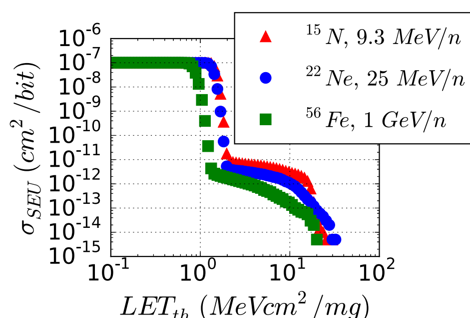

Fig. 5. Simulated cross section as a function of the LET threshold for different ions and energies per nucleon as simulated in FLUKA using the model presented in Section III.

model output on the assumed SV thickness is weak. For instance, for 230 MeV protons, the simulated cross section difference between a 0.1 and 1 μm thickness is only around 10% The model output does however strongly depend on the considered response function.

In addition, results from the SIMPA model available in the OMERE online tool [24] are shown included in the plot for the same HI cross section and SV thickness. As can be seen, the SIMPA output underestimates that from FLUKA and the experimental data by a factor $\sim$ 3. In addition, and though not explicitly shown in the present work, SIMPA also fails to reproduce the ESA Monitor SEU cross section increase in the 200 MeV - 3 GeV energy range published in [25] and reproduced in the FLUKA model, as it only yields the proton cross section up to an energy of 280 MeV. More generally, the SIMPA model does not take the contribution of high-Z materials into account, which can play a very strong role in the proton SEE cross section energy dependence in the several hundred MeV range [26], [27].

IV. Application to Sub-LET Threshold Region

Applying the approach introduced above to the sub-LET threshold region involves performing Monte Carlo simulations that include nucleus-nucleus interactions. In FLUKA, heavy ion transport was developed and implemented in 1998 [6]. However, the increasing demand for extending the FLUKA interaction models to heavy ions resulted in the adaptation and interfacing of the DPMJET code [28] for describing nucleus-nucleus collisions at accelerator and cosmic ray energies. DPMJET is based on the two component Dual Parton Model in connection with the Glauber formalism. It is used in FLUKA as nucleus-nucleus event generator for energies above 5 GeV/n, with the evaporation stage of excited residual nuclei performed in FLUKA. For energies below 5 GeV/n and above 100 MeV/n, FLUKA relies on a modified version of RQMD $-$ 2.4 which is a Relativistic Quantum Molecular Dynamic code [29]. Respective results can be found in [30], [31]. At even lower energies ($<$ 100 MeV/n) a treatment based on the Boltzmann Master Equation (BME) has been implemented [32]. In this regime, reactions are dominated by the fusion of the projectile and target ion, either through the so-called complete fusion (involving full momentum transfer) or break-up fusion, in which some part of the projectile and target behaves as a spectator while the reminder fuses in a composite system. In order to close the brief description of the nucleus-nucleus reactions in FLUKA, it is worth noting that a model for electromagnetic dissociation of ions is implemented since 2004 [33].

After having briefly described the ion-ion models, we apply the simulation procedure introduced in Section III for protons to HI in the sub-LET threshold region. The output of the calculations are the event-by-event energy deposition distributions which, if integrated as a function of the deposited energy yield the SEU probability as a function of the threshold energy. As shown in Fig. 3, we do not follow a pure threshold approach (i.e. step-function response) but rather fold the differential energy deposition distribution with the calibrated response function. However, for illustration purposes, we show the results for several of the simulated cases as the SEU cross section as a function of the threshold LET (i.e. assuming a response function with an onset at the different LET values). The results for three of the ions and energies considered are shown in Fig. 5, covering an energy interval of 9.3 MeV/n - 1 GeV/n.

Reading the graph from left to right, for low LET threshold values ($<$ 1 MeV cm^2/mg) the simulated cross sections for all ions correspond to the physical surface of the considered SV (10 μm^2), consistent with the fact that all ions reaching the surface deposit an energy above threshold. Between 1 and 2 MeV cm^2/mg, there is a fall-off of several orders of magnitude related to the fact that the LET threshold becomes larger than the LET of the ions and therefore only indirect energy deposition events can lead to an SEU. Above $\sim$ 2 MeV cm^2/mg, the respective cross sections correspond to events deriving from nuclear reactions. In this region, it is observed that for LET threshold values below $\sim$ 20 MeV cm^2/mg and the ions considered, the cross section is expected to decrease with increasing ion energy. It is only in a narrow LET threshold window ($\sim$ 20 $-$ 25 MeV cm^2/mg) in which the 25 MeV/n ion shows a larger cross section than the other two cases. It is worth reminding at this stage that, as shown in Fig. 5, the best fit of the LET threshold to the experimental data for the ESA SEU Monitor was 3.0 MeV cm^2/mg. Moreover, similar simulation results showing that the cross section is not expected to increase between 10 and 25 MeV/n are shown in [2].

The simulated cross section results using the response function described in Eq. (1) and Table II (i.e. same one as for the

Authorized licensed use limited to: University of Groningen. Downloaded on October 02,2020 at 07:56:07 UTC from IEEE Xplore. Restrictions apply.

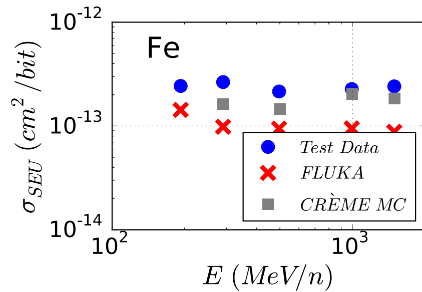

Fig. 6. Simulated SEU cross sections for Fe ions as a function of ion energy compared to experimental results.

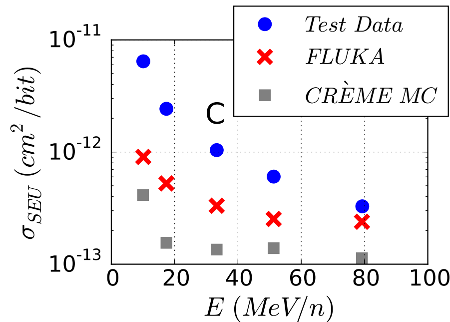

Fig. 7. Simulated SEU cross sections for C ions as a function of ion energy compared to experimental results.

protons) are plotted in Figs. 6, 7 and 8 for Fe, C and Ne respectively together with the experimental data. Error bars are not included as both those associated with the measurements (count error) and simulations (statistical uncertainty) are below 10% and therefore significantly smaller than the differences we are interested in analyzing. Both FLUKA and CRÈME MC were used as Monte Carlo simulation tools, however we first concentrate our analysis on results from the former, which are represented with red crossed in the plots.

As can be seen in Fig. 6, the high energy simulated Fe results (E $>$ 100 MeV/n) are in relatively good agreement with the data, with an underestimation of a factor $\sim$ $2-3$. As to what regards the C ion (Fig. 7), simulations underestimate the measurements by a factor $\sim$ 7 at 10 MeV/n with differences gradually reducing until finding a suitable agreement for an energy of 80 MeV/n. Furthermore, in the case of Ne (10 MeV/n $<$ E $<$ 30 MeV/n, Fig. 8), the simulated results underestimate the experimental results by a factor $\sim$ 7 at 10 MeV/n and over a factor 400 at 30 MeV/n, and fail to reproduce the strong experimental cross section increase in this energy range. It is to be underlined that a similar dependency has been previously identified for other components [15] and that a comparable underestimation for the 40 MeV/n Ar ion point was shown in [4] for SRAM#3 at the TAMU facility. Several possible explanations as to why simulations are not able to reproduce the HI experimental data in this energy range are discussed in detail in the following sections.

In addition to the FLUKA simulation results presented, the Geant4-based CRÈME MC online tool [34] was used in an analogous way (i.e. to retrieve the energy deposition distributions and fold them with the response function). The MRED version employed was mred $-$ 930 and at least $5 \cdot 10^6$ primaries were

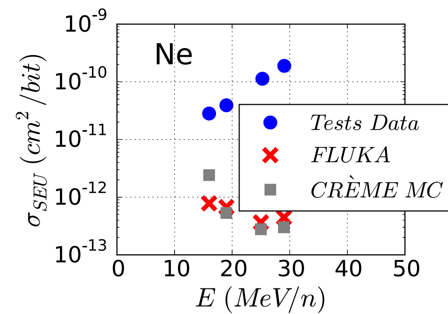

Fig. 8. Simulated SEU cross sections for Ne ions as a function of ion energy compared to experimental results.

simulated for each ion using the simplified secondary electron computation mode (recommended when the focus is on nuclear reaction events) and enabling nuclear processes. In all cases, a multiplicative factor of $\sim$ 700 for enhancing hadronic cross sections was automatically applied by the code. As can be noticed, the simulated output for both codes is: (i) compatible in the case of Ne (though the CRÈME MC result is factor $\sim$ 3 larger for 16 MeV/n); (ii) larger with FLUKA by a factor 2-3 for C; (iii) larger with CRÈME MC by a factor $\sim$ 3 for Fe.

It is worth noting that CRÈME MC was also used to obtain the expected proton SEU cross section in the 150-480 MeV range, yielding results which were 20 - 30% lower than the respective FLUKA values shown in Fig. 4.

V. Possible Sources of Underestimation

In our attempt to determine the sources of discrepancy between simulated and experimental results, we first of all concentrate on the impact of the SEU model parameters on the calculated cross sections. One of the simulation inputs to which the cross section output could be sensitive to is the assumed SV thickness. However, for protons of 230 MeV, ^{13}C of 10 MeV/n and ^{56}Fe of 1 GeV/n, calculations we performed showed that the cross section values in a thickness interval of $0.1-2$ μm are well within a factor 2, thus confirming the weak impact of this parameter on the model output.

Moreover, when analyzing the reaction probability and fragment production properties of the interactions relevant to this study, it is worth noting that whereas the reaction cross section in silicon for a given energy does not significantly increase with the mass number (A) of the ion (being only several factors larger than that of protons), the energy transferred to the fragment (and accordingly their range) is significantly larger for higher A and energy values [35]. Therefore, one of the possible explanations to the underestimation is that the geometry considered does not include elements that are still relevant in terms of fragment production potentially reaching the SV. This first obvious element is the air through which the ions travel before reaching the SV. Experiments at RADEF and UCL are performed in vacuum, however test setups at TAMU, GSI and KVI typically have a certain thickness of air between the vacuum pipe and the Device Under Test (DUT) [13]. For example, this distance corresponded to 80 mm in the tests performed at KVI. In our calculations however, no observable differences in the simulated cross section for 25 MeV/n ^{22}Ne ions were observed up to an

Authorized licensed use limited to: University of Groningen. Downloaded on October 02,2020 at 07:56:07 UTC from IEEE Xplore. Restrictions apply.

air thickness of 10 cm. In contrast, a $\sim 50\%$ increase was calculated with respect to the vacuum case for 30 mm of air and the 9.3 MeV/n ^{15}N ions. The analysis of the effect of fragments generated in other elements such as degraders and the vacuum exit window will be described in Section VI.

Likewise, the lateral size of the beam and the geometry surrounding the SV can also have an impact on the results. The simulations presented here were performed with a lateral beam and geometry size of $40 \times 40\ \mu\text{m}^2$. Whereas smaller beam sizes result in reduced cross sections for the different ions (up to a factor ~ 4 for $5 \times 5\ \mu\text{m}^2$) values for a surface of $200 \times 200\ \mu\text{m}^2$ are equivalent within statistical precision to those corresponding to $40 \times 40\ \mu\text{m}^2$. Therefore, the size used in our simulations can be considered as large enough to account for the effects of secondary particles reaching the SV from the sides.

As to what regards the materials surrounding the SV, only silicon, aluminum and silicon dioxide were considered, according to the BEOL information provided by the manufacturer. However, as has been previously shown [2], small tungsten elements near the SV are capable of significantly increasing the deposited energy through nuclear interactions, also in the case of heavy ions. Therefore, we included a thin, 50 nm tungsten slab directly on top of the SV, which for a cell surface of 10 μm^2 represents a tungsten volume of 0.5 μm^3, found to be representative for several commercial SRAM components of the 180 nm technology node [36]. We found that, both for 25 MeV/n ^{20}Ne and 1 GeV/n ^{56}Fe, tungsten only plays a role for LET thresholds above ~ 20 MeV cm^2/mg, and is therefore not relevant for the ESA SEU Monitor case.

From an experimental point of view, pulse-hight measurements were performed using in PIN diode under the different test conditions evidencing that the heavy ion beams employed did not have any visible contamination from other ion species and energies. This is an important result as even a very small fraction of contamination from an above-threshold ion could have a significant impact on the sub-LET threshold measurement.

VI. Effect of Beam Elements

The simulation model applied in Section IV considered the interaction of the heavy ion beams directly with the memory die, i.e. the only material included before the sensitive volume was the SRAM's BEOL (6.7 μm of Al and SiO_2). In this Section we will evaluate the impact of fragments produced in beam line elements such as the vacuum exit window, the air between it and the DUT, and the degraders used to alter the beam's energy and LET.

Before presenting the results of this analysis, it is worth mentioning that the simulation approach used here differs slightly from that introduced in Section III, in which the simulated cross section was derived by folding the energy deposition distribution in an SV of micro-metric dimensions with the HI response above the LET threshold. Proceeding analogously when beam elements in the cm scale are included can be challenging from a computational point of view, as the scoring region is orders of magnitude smaller than the overall geometry, thus rendering the simulation highly inefficient. For this reason, instead of scoring the energy deposition in a comparatively very small region, the approach we used was to score the LET of the particles on a surface directly above the SVs and of dimensions comparable to the full geometry considered. The resulting distribution was found to be fully compatible with the one obtained by dividing the energy deposition distribution by the SV depth. This fact evidences that the energy deposition for the cases studied (Ne beam between 15 and 29 MeV/n) is dominated by fragments produced outside the SV and for which the LET values do not significantly change in the path through the volume and are therefore representative of the energy deposition. It is to be noted that in the case of protons or higher energy (several hundred MeV range) heavy ions, we found the LET scoring approach significantly underestimated the actual energy deposition distribution, evidencing that fragments and recoils produced in the actual SV played a much more important role. Therefore, in these cases only results extracted from energy deposition distribution scoring are considered. Moreover, the CPU efficiency of the LET scoring approach is not only limited to the geometrical consideration introduced above, but can also be further optimized by (i) excluding the transport of the electromagnetic part (electrons, positrons and photons) (ii) introducing biasing factors for inelastic interactions, which is not an option directly available in the customized routines we use for the event-by-event energy deposition scoring.

The cases considered in order to quantify the analysis of the beam elements on the SEU cross section were the following:

1) A 29 MeV/n ^{20}Ne beam (i.e. same case as that in Section IV but scoring LET instead of deposited energy);
2) A 30 MeV/n ^{20}Ne beam traveling through 50 μm of Aramica exit window and 80 mm of air and reaching the DUT with an average energy of 29 MeV/n according to the information provided by the facility;
3) A 30 MeV/n ^{20}Ne beam traveling through 50 μm of Aramica exit window, 65 mm of air and 300, 700 and 800 μm of polyester degraders (density of 1.37 g/cm^3) and another 15 mm of air, reaching the DUT with an average energy of 25, 19 and 16 MeV/n respectively according to the information provided by the facility.

The resulting cross section values are plotted in Fig. 9 together with those corresponding to the energy deposition approach (shown in Section IV and not considering the beam elements introduced here). As can be seen, the effect on the SEU cross section of explicitly introducing the beam line elements is that of increasing its value for decreasing beam energy (i.e. increasing degrader thickness). This effect can be attributed to (i) the generation of secondary fragments in the beam line elements and (ii) the slowing down of such fragments, resulting in an increased LET. Therefore, it is important to note that, for the ion and energy range considered and the sub-LET threshold region, the expected impact of the degraders is stronger due to the fragment generation and slowing down than to the actual energy change of the primary beam. However, the consideration of the beam elements in the model geometry fails to explain the discrepancy between simulated and experimental data, especially at energies around 30 MeV/n.

For the C ion, the effect of the diffuser, exit window, air and degraders was not analyzed through simulations, however it is

Authorized licensed use limited to: University of Groningen. Downloaded on October 02,2020 at 07:56:07 UTC from IEEE Xplore. Restrictions apply.

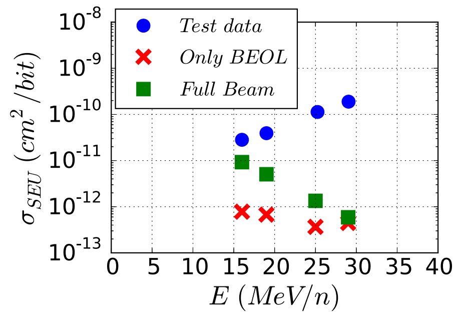

Fig. 9. Simulated sub-LET threshold Ne SEU cross sections as a function of ion energy compared to experimental results. Both a geometry including only the BEOL of the component and full beam line geometry are considered in the simulation.

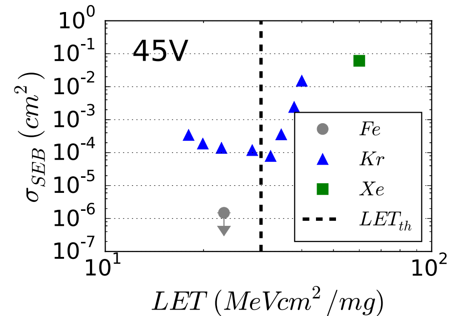

Fig. 10. Heavy ion SEB data as a function of LET for the power MOSFET biased at 45 V. All values were obtained with at least 50 events except for Fe, for which no events were observed and corresponds to the two-sigma upper limit.

worth noting that the following elements were present in the beam line:

1) A 0.3 mm lead diffuser to increase the size of the beam;
2) the 50 μm Aramica exit window;
3) 3 m of air;
4) Aluminum degraders of 4.5 mm for 53 MeV/n, 6.5 mm for 33 MeV/n and 7.7 mm for 17 MeV/n.

According to the results for the Ne ion, it is reasonable to expect that the beam elements introduced above could have a significant impact on the simulated C ion data set, potentially rendering it more compatible with the measured results (see Fig. 7). However, it is also to be noted that the lowest energy ion (10 MeV/n) corresponds to UCL and was taken in vacuum, therefore in this case the beam elements are not expected to account for the simulation underestimation.

VII. SEB Energy Dependency in Power MOSFET

The ESA SEU Monitor is an attractive component for the study of the energy dependency in the sub-LET threshold SEE cross section owing to its simplicity and extended use in a broad range of test facilities. However, the fact it has a relatively low LET threshold ($\sim$ 3 MeV $\mathrm{cm}^2/\mathrm{mg}$) implies that first of all, the LET region below threshold is only experimentally accessible to a limited amount of ions and energies and secondly, the potential effect of such interval will always be dominated by direct ionization in an interplanetary environment. For this reason, we have included a second component in our analysis, with the main interest of having a much larger LET threshold and being subject of an effect which is destructive and therefore critical for space mission planning.

The concerned component is the SFRI130.5 Vertical Diffused MOSFET (VDMOS) from Solid State Devices, Inc. (SSDI). The component was initially tested at the Lawrence Berkeley National Laboratory (LBNL) by a group from NASA [37]. The part was biased up to $\mathrm{V_{DS}} = 100\mathrm{V}$ (maximum rating) and was irradiated with 10 MeV/n argon and krypton ions. The part was found to be immune to Single Event Gate Rupture (SEGR) but suffered Single Event Burnout (SEB) before reaching a fluence of $5 \cdot 10^5$ ions/cm^2 for both ion species. $\mathrm{V_{DS}}$ was incremented in steps of 10 V and the last passing conditions were found to be 60 V for the Ar ion (LET $=$ 9.7 MeV $\mathrm{cm}^2/\mathrm{mg}$) and 40 V for the Kr one (LET $=$ 31 MeV $\mathrm{cm}^2/\mathrm{mg}$). These results were found to be independent of $\mathrm{V_{GS}}$, which was modified between 0 and -20 V.

In addition, measurements were performed on the same component by a group from ESA at the KVI test facility in Groningen, the Netherlands, as well as RADEF in Jyvaskyla, Finland. Test results were collected for biases of 45, 60, 75 and 100 V, however our analysis concentrates on the two first as they are the most revealing in terms of sub-LET threshold behaviour. As we will later show, the LET threshold for such conditions is estimated to be $\sim$ 25 MeV $\mathrm{cm}^2/\mathrm{mg}$ for 60 V and $\sim$ 30 MeV $\mathrm{cm}^2/\mathrm{mg}$ for 45 V. This means that both values are near the so-called iron knee, after which the GCR LET spectrum decreases significantly. Therefore, SEBs deriving from nuclear interactions can potentially have a large impact on the in-flight failure rate, thus rendering the analysis particularly relevant.

The SEB measurements were performed through a non-destructive approach in order to obtain statistically meaningful count values for the cross section derivation. The resistance in the drain path was set to 10 kΩ to avoid destructive burnout and the transient voltage drops when SEBs occurred were measured though a capacitor on the 1 MΩ input of an oscilloscope. Measurements were carried out on two DUTs for each experimental condition as a consistency check.

At both facilities (KVI and RADEF) degraders were used to obtain a broader range of ion energies and LETs. The details of such degraders are shown in Table III. The test results for both biases considered are shown in Tables IV and V. The horizontal line in the middle of the table represents the transition between sub-LET and above-LET threshold cross sections. The former results are ordered by energy per nucleon whereas the latter are presented in increasing LET. Moreover, results are plotted in Figs. 10 and 11 as a function of LET.

As was the case for the ESA Monitor results introduced in Section II, the cross section points above the LET threshold show a well-behaved trend regardless of the ion species and energy. Contrarily, below the threshold, LET is no longer a relevant figure-of-merit to describe the SEE cross section.

In order to have a more direct insight of the energy and ion species dependency of the SEB cross section in the sub-LET threshold region, Figs. 12 and 13 show the corresponding values as a function of ion energy for the 45 and 60 V bias respectively. In the case of the first, there is a moderate increase with energy

Authorized licensed use limited to: University of Groningen. Downloaded on October 02,2020 at 07:56:07 UTC from IEEE Xplore. Restrictions apply.

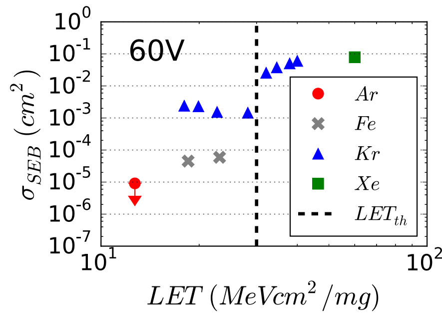

Fig. 11. Heavy ion SEB data as a function of LET for the power MOSFET biased at 60 V. All values were obtained with at least 50 events except for Ar, for which no events were observed and corresponds to the two-sigma upper limit.

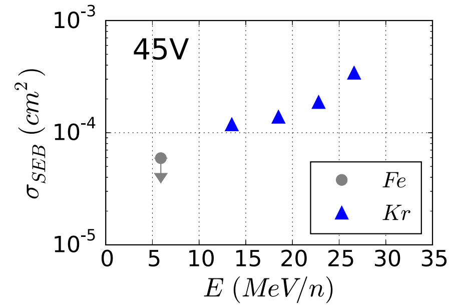

Fig. 12. Heavy ion SEB data in the sub-LET threshold region as a function of energy for the power MOSFET biased at 45 V. All values were obtained with at least 50 events except for Fe, for which no events were observed and corresponds to the two-sigma upper limit.

TABLE III
DEGRADER DETAILS FOR SEB TESTS AT RADEF AND KVI

Facility	Ion	Deg. Material	Deg. Thickness (μm)	Energy (MeV/n)	LET (MeVcm^2/mg)
RADEF	^{56}Fe	Kapton-Mylar	50	5.9	23.1
RADEF	^{82}Kr	Kapton-Mylar	50	5.4	37.9
KVI	^{40}Ar	Kapton	725	5.3	12.7
KVI	^{84}Kr	Polyester	100	22.8	19.9
KVI	^{84}Kr	Polyester	200	18.5	22.7
KVI	^{84}Kr	Polyester	300	13.5	28.2
KVI	^{84}Kr	Polyester-Kapton	375	8.9	34.6
KVI	^{84}Kr	Polyester-Kapton	425	5.4	40.0

TABLE IV
SEB HEAVY ION DATA FOR THE SSDI-SFRI130.5 POWER MOSFET BIASED AT 45 V

Facility	Ion	Energy (MeV/n)	LET (MeVcm^2/mg)	σ_{SEB} (cm^2/bit)
RADEF	^{56}Fe	5.9	23.1	$< 1.49 \cdot 10^{-6}$
KVI	^{84}Kr	13.5	28.2	$1.19 \cdot 10^{-4}$
KVI	^{84}Kr	18.5	22.7	$1.39 \cdot 10^{-4}$
KVI	^{84}Kr	22.8	19.9	$1.88 \cdot 10^{-4}$
KVI	^{84}Kr	26.6	18.0	$3.43 \cdot 10^{-4}$
RADEF	^{82}Kr	9.4	32.1	$7.90 \cdot 10^{-5}$
KVI	^{84}Kr	8.9	34.6	$3.58 \cdot 10^{-4}$
RADEF	^{82}Kr	5.4	37.9	$2.42 \cdot 10^{-3}$
KVI	^{84}Kr	5.4	40.0	$1.52 \cdot 10^{-2}$
RADEF	^{131}Xe	9.3	60.0	$6.10 \cdot 10^{-2}$

TABLE V
SEB HEAVY ION DATA FOR THE SSDI-SFRI130.5 POWER MOSFET BIASED AT 60 V

Facility	Ion	Energy (MeV/n)	LET (MeVcm^2/mg)	σ_{SEB} (cm^2/bit)
KVI	^{40}Ar	5.3	12.7	$< 9.09 \cdot 10^{-6}$
RADEF	^{56}Fe	5.9	23.1	$5.93 \cdot 10^{-5}$
RADEF	^{56}Fe	9.3	18.5	$4.51 \cdot 10^{-5}$
KVI	^{84}Kr	18.5	22.7	$1.54 \cdot 10^{-3}$
KVI	^{84}Kr	22.8	19.9	$2.32 \cdot 10^{-3}$
KVI	^{84}Kr	26.6	18.0	$2.41 \cdot 10^{-3}$
KVI	^{84}Kr	13.5	28.2	$1.46 \cdot 10^{-3}$
RADEF	^{82}Kr	9.4	32.1	$2.57 \cdot 10^{-2}$
KVI	^{84}Kr	8.9	34.6	$3.79 \cdot 10^{-2}$
RADEF	^{82}Kr	5.4	37.9	$5.04 \cdot 10^{-2}$
KVI	^{84}Kr	5.4	40.0	$6.05 \cdot 10^{-2}$
RADEF	^{131}Xe	9.3	60.0	$7.84 \cdot 10^{-2}$

for the Kr ion, with the cross section augmenting a factor $\sim$ 3 between 13.5 and 26.6 MeV/n. This increase is comparable (though weaker) than that observed for the ESA Monitor and

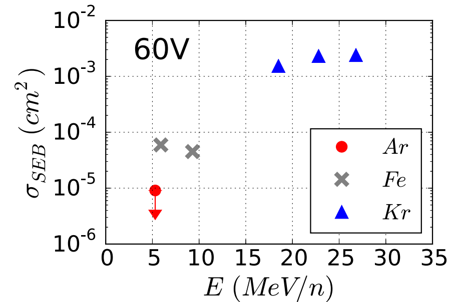

Fig. 13. Heavy ion SEB data in the sub-LET threshold region as a function of energy for the power MOSFET biased at 60 V. All values were obtained with at least 50 events except for Ar, for which no events were observed and corresponds to the two-sigma upper limit.

Ne ion between 16 and 29 MeV/n, also at KVI. Moreover, the measurement with the Fe ion at an energy of 5.9 MeV/n only provided an upper limit to the cross section, as no SEBs were observed.

In the case of the 60 V, the cross section increase for Kr between 18.5 and 26.6 is below a factor 2. Moreover, unlike the case for the 45 V bias, Fe ions at RADEF were capable of inducing SEBs, with comparable cross sections at 5.9 and 9.3 MeV/n. However, this should not be taken as a conclusive result that the Fe sub-LET threshold cross section has a weak dependency with energy in this range as (i) the 5.9 MeV/n has an LET value very close to the estimated LET threshold, and can therefore (at least partially) still be affected by direct ionization from the primary beam (ii) fragments from the degrader used to decrease the energy from 9.3 down to 5.9 MeV/n could play a significant role on the measured cross section. In addition, the Ar measurement at 5.3 MeV/n only yielded an upper limit to the cross section. However, it is to be noted at this point that 60 V was the last value for which the same reference passed the $5 \cdot 10^5$ ion/cm^2 test with the 10 MeV/n Ar beam at LBNL, therefore it is likely that the part could also fail due to sub-LET threshold Ar ions at a larger energy or fluence than those tested for at KVI. Furthermore, despite the fact the Fe and Kr data do not overlap in energy, the difference of over an order of magnitude between the results corresponding to each ion suggest that, in addition to the energy dependence and as reported in [13], the ion species also plays a very important role in the sub-LET threshold cross section.

Authorized licensed use limited to: University of Groningen. Downloaded on October 02,2020 at 07:56:07 UTC from IEEE Xplore. Restrictions apply.

VIII. Conclusions and Future Work

From an experimental point of view, the three main conclusions of the work we present here are:

(i) the confirmation through SEU and SEB measurements of the sub-LET threshold cross section increase with energy in the 10-30 MeV/n region for Ne and Kr ions respectively, including measurements in the new HI facility at KVI;

(ii) the observation of an opposite trend for C in the 10-80 MeV/n, with the cross section decreasing as a function of increasing energy;

(iii) the significant decrease of the sub-LET threshold SEU cross section between 30 and 200 MeV/n when considering the combined C and Fe results, and a relatively constant behavior up to 1.5 GeV/n.

From a simulation standpoint, this work shows that Monte Carlo simulations of the SEU cross section using a model calibrated to the above threshold heavy ion response is successful in reproducing the proton and high energy ($>$ 80 MeV/n) HI test data within a factor 3, but significantly underestimates the test results in the 10-30 MeV/n range for C and Ne. In the case of the latter, the disagreement is particularly relevant, as while simulations expect a relatively constant cross section in this range (or even a decreasing one if the effect of the secondaries produced in the degrader is explicitly considered) measurements at both KVI and TAMU show an abrupt increase.

Different sources of discrepancy are explored related to the parameters of the model, including the SV thickness, the materials through which the ions travel, the size of the beam and geometry, and the impact of beam line elements. Results show that the effect of such possible sources is limited when compared to the differences between the simulated and experimental cross section values (with the exception of the degrader impact for Ne points near 15 MeV/n). Because Monte Carlo simulation codes are an essential tool to estimate the contribution of the sub-LET threshold region to the overall SEE rate, we consider it is important to understand the source(s) of underestimation and (if possible) correct it (them) in order to obtain realistic predictions.

In addition, despite the mismatch between simulations and experiments around 30 MeV/n, the fact that the simulated SEU cross section for the 16 MeV/n ^{20}Ne ion is a factor $\sim$ 10 larger when considering the actual transport and interaction of the beam through the degrader suggests that elements of this type should be carefully taken into account in Monte Carlo simulations focused on the sub-LET threshold region. For this reason, tests performed in vacuum and with a minimal amount of elements in the trajectory of the beam are preferred for sub-LET threshold analyses, as otherwise uncoupling the effect of the primary beam and fragment contribution can be challenging.

Moreover, with the purpose of extending the conclusions on the impact of the ion species and energy in the sub-LET threshold region, we intend to broaden the experimental result set to other components and SEE types. The enhanced analysis will include components for which high-Z materials have shown to play an important role for proton-induced SEE cross sections [26], [36] and which are also expected to have a significant impact in the case of heavy ions in the sub-LET threshold region [2], [3], [15].

In parallel to the experimental line of research, efforts will be devoted to investigate the discrepancy between measurements and Monte Carlo based simulations, as the latter are an essential ingredient to determine the impact of the sub-LET threshold region in a systematic manner. One of the points that will be investigated is the impact of the effective charge of the secondary ions (typically considered as average values in Monte Carlo codes, but actually following a distribution) on the event-by-event energy deposition distribution.

References

[1] R. Ecoffet and S. Duzellier, “Estimation of latch-up sensitive thickness and critical energy using large inclination heavy ion beams,” *IEEE Trans. Nucl. Sci.*, vol. 44, no. 6, pp. 2378–2385, Dec. 1997.

[2] C. L. Howe, R. A. Weller, R. A. Reed, M. H. Mendenhall, R. D. Schrimpf, K. M. Warren, D. R. Ball, L. W. Massengill, K. A. LaBel, J. Howard, J. W. , and N. F. Haddad, “Role of heavy-ion nuclear reactions in determining on-orbit single event error rates,” *IEEE Trans. Nucl. Sci.*, vol. 52, no. 6, pp. 2182–2188, Dec. 2005.

[3] K. M. Warren, R. A. Weller, M. H. Mendenhall, R. A. Reed, D. R. Ball, C. L. Howe, B. D. Olson, M. L. Alles, L. W. Massengill, R. D. Schrimpf, N. F. Haddad, S. E. Doyle, D. McMorrow, J. S. Melinger, and W. T. Lotshaw, “The contribution of nuclear reactions to heavy ion single event upset cross-section measurements in a high-density SEU hardened SRAM,” *IEEE Trans. Nucl. Sci.*, vol. 52, no. 6, pp. 2125–2131, Dec. 2005.

[4] R. A. Reed, R. A. Weller, M. H. Mendenhall, J.-M. Lauenstein, K. M. Warren, J. A. Pellish, R. D. Schrimpf, B. D. Sierawski, L. W. Massengill, P. E. Dodd, M. R. Shaneyfelt, J. A. Felix, J. R. Schwank, N. F. Haddad, R. K. Lawrence, J. H. Bowman, and R. Conde, “Impact of ion energy and species on single event effects analysis,” *IEEE Trans. Nucl. Sci.*, vol. 54, no. 6, pp. 2312–2321, Dec. 2007.

[5] Texas A&M university cyclotron institute radiation effects facility website [Online]. Available: http://cyclotron.tamu.edu/ref/

[6] A. Ferrari, P. R. Sala, A. Fasso, and J. Ranft, FLUKA, a multi-particle transport code CERN-2005-10-2005, INFN/TC-05/11, SLAC-R-773, 2005.

[7] G. Battistoni, S. Muraro, P. R. Sala, F. Cerruti, A. Ferrari, S. Roesler, A. Fasso, and J. Ranft, “The FLUKA code: Description and benchmarking,” presented at the Hadronic Shower Simulation Workshop, Batavia, IL, USA, Sep. 6–8, 2006.

[8] F. Ballarini, G. Battistoni, M. Brugger, M. Campanella, M. Carboni, F. Cerutti, A. Empl, A. Fasso, A. Ferrari, E. Gadioli, M. Garzelli, M. Lantz, A. Mairani, A. Mostacci, S. Muraro, A. Ottolenghi, V. Patera, M. Pelliccioni, L. Pinsky, J. Ranft, S. Roesler, P. Sala, D. Scannicchio, G. Smirnov, F. Sommerer, S. Trovati, R. Villari, V. Vlachoudis, T. Wilson, and N. Zapp, “The physics of the FLUKA code: Recent developments,” *Advances Space Res.*, vol. 40, no. 9, pp. 1339–1349, 2007 [Online]. Available: http://www.sciencedirect.com/science/article/pii/S0273117707004905

[9] R. Harboe-Sorensen, F.-X. Guerre, and A. Roseng, “Design, testing and calibration of a reference SEU monitor system,” in *Proc. 8th Eur. Conf. on Radiation and its Effects on Components and Systems*, Sep. 2005, pp. B3-1–B3-7.

[10] R. Harboe-Sorensen, C. Poivey, F.-X. Guerre, A. Roseng, F. Lochon, G. Berger, W. Hajdas, A. Virtanen, H. Kettunen, and S. Duzellier, “From the reference SEU monitor to the technology demonstration module on-board PROBA-II,” *IEEE Trans. Nucl. Sci.*, vol. 55, no. 6, pp. 3082–3087, Dec. 2008.

[11] R. Harboe-Sorensen, C. Poivey, N. Fleurinck, K. Puimege, A. Zadeh, F.-X. Guerre, F. Lochon, M. Kaddour, L. Li, D. Walter, A. Keating, A. Jaksic, and M. Poizat, “The technology demonstration module on-board PROBA-II,” *IEEE Trans. Nucl. Sci.*, vol. 58, no. 3, pp. 1001–1007, Jun. 2011.

[12] R. Harboe-Sorensen, C. Poivey, A. Zadeh, A. Keating, N. Fleurinck, K. Puimege, F.-X. Guerre, F. Lochon, M. Kaddour, L. Li, and D. Walter, “PROBA-II technology demonstration module in-flight data analysis,” *IEEE Trans. Nucl. Sci.*, vol. 59, no. 4, pp. 1086–1091, Aug. 2012.

Authorized licensed use limited to: University of Groningen. Downloaded on October 02,2020 at 07:56:07 UTC from IEEE Xplore. Restrictions apply.

[13] V. Ferlet-Cavrois, J. R. Schwank, S. Liu, M. Muschitiello, T. Beutier, A. Javanainen, A. Hedlund, C. Poivey, A. Mohammadzadeh, R. Harboe-Sorensen, G. Santin, B. Nickson, A. Menicucci, C. Binois, D. Peyre, S. K. Hoeffgen, S. Metzger, D. Schardt, H. Kettunen, A. Virtanen, G. Berger, B. Piquet, J.-C. Foy, M. Zafrani, P. Truscott, M. Poizat, and F. Bezerra, "Influence of beam conditions and energy for SEE testing," *IEEE Trans. Nucl. Sci.*, vol. 59, no. 4, pp. 1149–1160, Aug. 2012.

[14] S. K. Hoeffgen, M. Durante, V. Ferlet-Cavrois, R. Harboe-Sorensen, W. Lennartz, T. Kuendgen, J. Kuhnhenn, C. LaTessa, M. Mathes, A. Menicucci, S. Metzger, P. Nieminen, R. Pleskac, C. Poivey, D. Schardt, and U. Weinand, "Investigations of single event effects with heavy ions of energies up to 1.5 GeV/n," *IEEE Trans. Nucl. Sci.*, vol. 59, no. 4, pp. 1161–1166, Aug. 2012.

[15] P. E. Dodd, J. R. Schwank, M. R. Shaneyfelt, J. A. Felix, P. Paillet, V. Ferlet-Cavrois, J. Baggio, R. A. Reed, K. M. Warren, R. A. Weller, R. D. Schrimpf, G. L. Hash, S. M. Dalton, K. Hirose, and H. Saito, "Impact of heavy ion energy and nuclear interactions on single-event upset and latchup in integrated circuits," *IEEE Trans. Nucl. Sci.*, vol. 54, no. 6, pp. 2303–2311, Dec. 2007.

[16] D. Lambert, F. Desnoyers, and D. Thouvenot, "Investigation of neutron and proton SEU cross-sections on SRAMs between a few Mev and 50 Mev," in *Proc. Eur. Conf. on Radiation and Its Effects on Components and Systems (RADECS)*, Sep. 2009, pp. 148–154.

[17] E. L. Petersen, V. Pouget, L. W. Massengill, S. P. Buchner, and D. McMorrow, "Rate predictions for single-event effects - critique II," *IEEE Trans. Nucl. Sci.*, vol. 52, no. 6, pp. 2158–2167, 2005.

[18] K. M. Warren, R. A. Weller, B. D. Sierawski, R. A. Reed, M. H. Mendenhall, R. D. Schrimpf, L. W. Massengill, M. E. Porter, J. D. Wilkinson, K. A. LaBel, and J. H. Adams, "Application of RADSAFE to model the single event upset response of a $0.25\ \mu$m CMOS SRAM," *IEEE Trans. Nucl. Sci.*, vol. 54, no. 4, pp. 898–903, Aug. 2007.

[19] B. D. Sierawski, J. A. Pellish, R. A. Reed, R. D. Schrimpf, K. M. Warren, R. A. Weller, M. H. Mendenhall, J. D. Black, A. D. Tipton, M. A. Xapsos, R. C. Baumann, X. Deng, M. J. Campola, M. R. Friendlich, H. S. Kim, A. M. Phan, and C. M. Seidleck, "Impact of low-energy proton induced upsets on test methods and rate predictions," *IEEE Trans. Nucl. Sci.*, vol. 56, no. 6, pp. 3085–3092, Dec. 2009.

[20] J. C. Pickel, "Single-event effects rate prediction," *IEEE Trans. Nucl. Sci.*, vol. 43, no. 2, pp. 483–495, Apr. 1996.

[21] B. Doucin, Y. Patin, J. P. Lochard, J. Beaucour, T. Carriere, D. Isabelle, J. Buisson, T. Corbiere, and T. Bion, "Characterization of proton interactions in electronic components," *IEEE Trans. Nucl. Sci.*, vol. 41, no. 3, pp. 593–600, Jun. 1994.

[22] B. Doucin, T. Carriere, C. Poivey, P. Garnier, J. Beaucour, and Y. Patin, "Model of single event upsets induced by space protons in electronic devices," in *Proc. 3rd Eur. Conf. on Radiation and its Effects on Components and Systems*, Sep. 1995, pp. 402–408.

[23] J. Barak, J. Levinson, A. Akkerman, Y. Lifshitz, and M. Victoria, "A simple model for calculating proton induced SEU," *IEEE Trans. Nucl. Sci.*, vol. 43, no. 3, pp. 979–984, Jun. 1996.

[24] "OMERE software TRAD tests and radiations," [Online]. Available: http://www.trad.fr/OMERE-Software.html

[25] R. G. Alia, M. Brugger, S. Danzeca, V. Ferlet-Cavrois, C. Poivey, K. Roed, F. Saigne, G. Spiezia, S. Uznanski, and F. Wrobel, "SEE measurements and simulations using mono-energetic GeV-energy hadron beams," *IEEE Trans. Nucl. Sci.*, vol. 60, no. 6, pp. 4142–4149, Dec. 2013.

[26] R. G. Alia, M. Brugger, S. Danzeca, V. Ferlet-Cavrois, C. Poivey, K. Roed, F. Saigne, G. Spiezia, S. Uznanski, and F. Saigne, "Energy dependence of tungsten-dominated SEL cross sections," *IEEE Trans. Nucl. Sci.*, vol. 61, no. 5, pp. 2718–2726, Oct. 2014.

[27] S. Uznanski, R. G. Alia, E. Blackmore, M. Brugger, R. Gaillard, J. Mekki, B. Todd, M. Trinczek, and A. Villanueva, "The effect of proton energy on SEU cross section of a 16 Mbit TFT PMOS SRAM with DRAM capacitors," *IEEE Trans. Nucl. Sci.*, vol. 61, no. 6, pp. 3074–3079, Dec. 2014.

[28] S. Roesler, R. Engel, and J. Ranft, "The Monte carlo event generator DPMJET-III," in *Proc. Advanced Monte Carlo for Radiation Physics, Particle Transport Simulation and Applications*, Lisbon, Portugal, Oct. 23–26, 2001, pp. 1033–1038.

[29] H. Sorge, H. Stöcker, and W. Greiner, "Poincaré invariant Hamiltonian dynamics: Modelling multi-hadronic interactions in a phase space approach," *Annals Phys.*, vol. 192, no. 2, pp. 266–306, 1989.

[30] V. Andersen, F. Ballarini, G. Battistoni, M. Campanella, M. Carboni, F. Cerutti, A. Empl, A. Fasso, A. Ferrari, and E. Gadioli *et al.*, "The FLUKA code for space applications: Recent developments," *Advances Space Res.*, vol. 34, no. 6, pp. 1302–1310, 2004.

[31] H. Aiginger, V. Andersen, F. Ballarini, G. Battistoni, M. Campanella, M. Carboni, F. Cerutti, A. Empl, W. Enghardt, and A. Fassò *et al.*, "The FLUKA code: New developments and application to 1 GeV/n iron beams," *Advances Space Res.*, vol. 35, no. 2, pp. 214–222, 2005.

[32] F. Cerutti, G. Battistoni, G. Capezzali, P. Colleoni, A. Ferrari, E. Gadioli, A. Mairani, and A. Pepe, "Low energy nucleus–nucleus reactions: The BME approach and its interface with FLUKA," presented at the 11th Int. Conf. on Nuclear Reaction Mechanisms, Varenna, Italy, Jun. 12–16, 2006.

[33] F. Ballarini, J. Ranft, L. S. Pinsky, A. Empl, P. Sala, G. Smirnov, A. Ferrari, G. Battistoni, E. Gadioli, and A. Fasso *et al.*, "Nuclear models in FLUKA: Present capabilities, open problems and future improvements," in *AIP Conf. Proc.*, 2004, vol. 769, no. SLAC-PUB-10813, pp. 1197–1202.

[34] "CREME site by the Vanderbilt University School of Engineering," [Online]. Available: https://creme.isde.vanderbilt.edu/

[35] C. Inguimbert, S. Duzellier, T. Nuns, and F. Bezerra, "Using subthreshold heavy ion upset cross section to calculate proton sensitivity," *IEEE Trans. Nucl. Sci.*, vol. 54, no. 6, pp. 2394–2399, Dec. 2007.

[36] R. G. Alia, E. W. Blackmore, M. Brugger, S. Danzeca, V. Ferlet-Cavrois, R. Gaillard, J. Mekki, C. Poivey, K. Roed, F. Saigne, G. Spiezia, M. Trinczek, S. Uznanski, and F. Wrobel, "SEL cross section energy dependence impact on the high energy accelerator failure rate," *IEEE Trans. Nucl. Sci.*, vol. 61, no. 6, pp. 2936–2944, Dec. 2014.

[37] J.-M. Lauenstein, A. D. Topper, M. C. Casey, E. P. Wilcox, A. M. Phan, H. S. Kim, and K. A. LaBel, "Recent radiation test results for power MOSFETs," in *Proc. IEEE Radiation Effects Data Workshop (REDW)*, Jul. 2013, pp. 1–6.

Authorized licensed use limited to: University of Groningen. Downloaded on October 02,2020 at 07:56:07 UTC from IEEE Xplore. Restrictions apply.